

We extend the saturation models *à la* Golec-Biernat and Wüsthoff to cross-sections of hard processes initiated by virtual-gluon probes separated by large rapidity intervals at hadron colliders. We derive their analytic expressions and apply them to physical examples, such as saturation effects for Mueller-Navelet forward jets. By comparison to $\gamma^* - \gamma^*$ cross-sections we find a more abrupt transition to saturation. We propose to study observables with a potentially clear saturation signal and to use heavy vector and flavored mesons as alternative hard probes to forward jets.

I. INTRODUCTION

The saturation regime describes the high-density phase of partons in perturbative QCD. It may occur for instance when the Balitsky-Fadin-Kuraev-Lipatov (BFKL) QCD evolution equation [1] goes beyond some energy limit [2, 3, 4, 5, 6, 7]. On a phenomenological ground, a well-known saturation model [8] by Golec-Biernat and Wüsthoff (GBW) gives a parametrisation of the proton structure functions already in the HERA energy range. It provides a simple and elegant formulation of the transition to saturation. However, there does not yet exist a clear confirmation of saturation since the same data can well be explained within the conventional perturbative QCD framework [9].

An interesting question is whether the experiments at high-energy hadron colliders, such as the Tevatron or LHC, can test saturation while for the moment this search is mainly considered for heavy-ion collisions. In the present paper, our aim is to look for saturation effects in the context of Mueller-Navelet [10] forward-jet production in hadron-induced hard collisions. The key difference with electron-induced reactions is that the hard probe is no more a virtual photon γ^* but a virtual gluon g^* , see Fig.1a.

A basic ingredient of the GBW saturation models is the QCD dipole formalism [11, 12] in which the hard cross-sections read

$$\sigma = \int d^2r_1 d^2r_2 \phi^{(1)}(r_1, Q_1^2) \phi^{(2)}(r_2, Q_2^2) \sigma_{dd}(\Delta\eta, r_1, r_2) , \quad (1)$$

where $r_{i=1,2}$ are the transverse sizes of the dipoles and $\Delta\eta$ is the pseudo-rapidity range of the dipole-dipole cross-section $\sigma_{dd}(\Delta\eta, r_1, r_2)$. In our notations, $\phi^{(i)}(r_i, Q_i^2)$ are the dipole distributions in the target and projectile, and Q_i the virtualities of the hard probes that set the perturbative scale.

Formula (1) expresses a factorization property which has been shown to be equivalent [13] to k_T -factorization [14] in the BFKL framework. In this framework, the distributions $\phi^{(i)}(r_i, Q_i^2)$ are related to the “impact factors” which describe the coupling of the target and projectile to the BFKL kernel. In the case of γ^* -induced reactions, the dipole distribution functions $\phi^\gamma(r, Q^2)$ are well-known from QED and the equivalence with photon impact factors checked. In the case of forward-jet production with transverse momentum $q_T \geq Q \gg 1 \text{ GeV}$, the corresponding distribution $\phi(r, Q^2)$ can be derived [15, 16] in the collinear approximation *i.e.* in the Double Leading Log approximation (DLL).

In the present paper, following an approach [17] for $\gamma^* - \gamma^*$ cross-sections, we shall describe the predictions of saturation for g^* -induced reactions such as Mueller-Navelet [10] forward-jet production. For this sake, we will make use of the dipole distribution $\phi(r, Q^2)$ derived in [15, 16]. For simplicity, we assume the validity of the same GBW cross-sections as for $\gamma^* - \gamma^*$. The k_T -factorization property is assumed to be preserved in the presence of saturation (see a recent discussion in [18]). The question of going beyond this simple scheme *e.g.* using a more complete formulation of saturation [19] is left for further work.

The plan of the paper is as follows. In section II, recalling the results of [15, 16], we show how the emission of a forward gluon jet can be recast in terms of a dipole distribution. We also present the GBW formulation of the dipole-dipole cross-sections. In section III, we derive our results for the Mueller-Navelet jets cross-sections with saturation. In section IV, we discuss these results in the prospect of experiments at the Tevatron and LHC and propose characteristic observables for saturation. The final section V is devoted to conclusion and outlook.

‡ URA 2306, unité de recherche associée au CNRS.

*Electronic address: marquet@spht.saclay.cea.fr

†Electronic address: pesch@spht.saclay.cea.fr

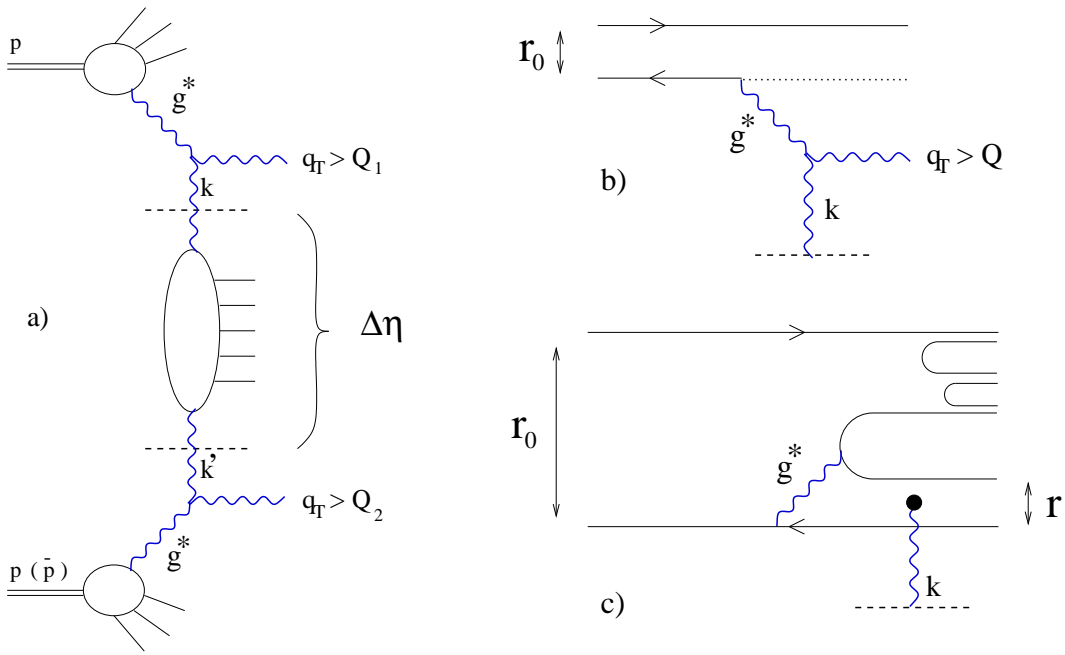


FIG. 1: *Forward jets and impact factors at hadron colliders.* Fig 1a: Mueller-Navelet jets at hadron colliders. Fig 1b: onium (+jet) impact factor in the partonic representation. Fig 1c: onium (+jet) impact factor in the dipole representation. $\Delta\eta$: rapidity gap between the two gluon jets. $q_T > Q_{1,2}$: transverse momenta of the gluon jets. k, k' : transverse momenta of the gluons interacting with the BFKL kernel. The gluon-dipole coupling ($f^0(k^2, r)$, see text) is sketched by the black point in Fig.1c.

II. DIPOLE FORMULATION

A. Forward jets and dipole distributions

Let us first recall how one can obtain the dipole distribution $\phi(r, Q^2)$ associated with a forward jet with transverse momentum $q_T > Q$. The derivation is made [16] using the example of a final-state gluon being emitted from an onium ($q\bar{q}$ state) of size r_0 , see Fig1b. QCD factorization will allow to extend the result to the case of an incident hadron.

Assuming the condition $1 \text{ GeV}^{-1} \gg r_0 \gg 1/Q$, the onium is small enough to allow a perturbative QCD calculation but large enough with respect to the inverse transverse momentum of the forward jet. Using k_T -factorization in the BFKL framework the (unintegrated) gluon density $f(k^2, r_0)$ entering at each vertex of the BFKL cross-section (see Fig.1b) can be factorized [16] in the following way:

$$f(k^2, r_0) \equiv \bar{\alpha} \log \frac{1}{x} \int \frac{d^2 \vec{q}}{\pi \vec{q}^2} \theta(\vec{q}^2 - Q^2) f^0(|\vec{k} + \vec{q}|^2, r_0) \approx \int_0^{r_0} d^2 r \left\{ 2\bar{\alpha} \log \frac{1}{x} \log \frac{r_0}{r} \right\} \frac{Q}{2\pi r} J_1(Qr) f^0(k^2, r) \quad (2)$$

in the collinear approximation $r_0 q_T \gg 1$ for the onium. k is the transverse momentum of the gluon connected to the BFKL kernel (see Fig.1). $f(k^2, r_0)$ is the lowest order BFKL equation written in an unfolded form (see for instance [20]) and the initial gluon density reads $f^0(k^2, r) \equiv 2\bar{\alpha}(1 - J_0(kr))/k^2$. J_0 and J_1 are the Bessel functions.

Equation (2) can be interpreted as the extension to forward jets of the equivalence [13] between the momentum-space (partonic) and coordinate-space (dipole) representations. The middle term corresponds to the contribution displayed in Fig.1b. The last term is described in Fig.1c and matches with the Mueller picture [12] of cascading dipoles in the $1/N_c$ limit, in which the QCD wave function of an initial onium is expanded over multi colorless-dipole configurations. The factor in brackets $\{2\bar{\alpha} \log \frac{1}{x} \log \frac{r_0}{r}\}$ corresponds to the first order contribution of the Dokshitzer-Gribov-Lipatov-Altarelli-Parisi (DGLAP) gluon ladder [9], *i.e.* the probability of finding a dipole of size r inside the onium of size r_0 , at the Double Leading Log (DLL) approximation; thanks to QCD factorization properties, it is included in the gluon structure function of the incident particle. $f^0(k^2, r)$ is nothing else than the factorized gluon density [12, 21] inside the dipole of size r which, in the dipole formulation (1) is included in the dipole-dipole cross-section.

Having factorized out both the contribution to the structure function and the one to the dipole-dipole cross-section, one is left with the function $\phi(r, Q^2)$ which describes the resulting size distribution of the interacting dipole. Hence,

one is led to identify¹

$$\phi(r, Q^2) \equiv \frac{Q}{2\pi r} J_1(Qr) . \quad (3)$$

The forward-jet emission is thus put in correspondence with a small colorless dipole of size $r = \mathcal{O}(1/Q)$. The distribution of sizes around that value is given by $\phi(r, Q^2)$ in (3).

Some comments are in order. Via its description in terms of dipoles, k_T -factorization leads to a description of the forward jet (coming from a colorful virtual gluon g^*) in terms of colorless $q\bar{q}$ dipoles. Indeed, within the $1/N_c$ scheme of the dipole formalism, the color neutralization of the forward jet is described by a cascade of dipoles, as pictured in Fig.1c. This means that, in this representation, the color quantum number carried by the *incoming* virtual gluon g^* is neutralized through the cascade of dipoles.

The obtained dipole distribution $\phi(r, Q^2)$ is not everywhere positive, the Bessel function oscillating in sign for $rQ \gtrsim 4$, and therefore cannot be interpreted as a probability distribution. We interpret this feature as a breakdown of the collinear approximation. Hence, in our framework, we have to check the positivity of the cross-sections, as will be discussed later on. For the Mueller-Navelet BFKL cross-section, positivity is satisfied by construction.

B. Dipole-dipole cross-sections with saturation

Let us recall the formulation of the GBW saturation model for dipole collisions. Initially, the GBW approach [8] is a model for the dipole-proton cross-section which includes the saturation damping of large-dipole configurations. For the description of $\gamma^* - \gamma^*$ cross-sections at LEP, see Ref. [17], it has been extended² to dipole-dipole cross-sections. The same saturation scale is considered for dipole-dipole and dipole-proton cross-sections.

The parametrisation of this dipole-dipole cross-section is

$$\sigma_{dd}(\Delta\eta, r_1, r_2) = \sigma_0 \left\{ 1 - \exp\left(-\frac{r_{\text{eff}}^2}{4R_0^2(\Delta\eta)}\right) \right\}, \quad (4)$$

where $R_0(\Delta\eta) = e^{-\frac{\lambda}{2}(\Delta\eta - \Delta\eta_0)}/Q_0$ is the rapidity-dependent saturation radius and the dipole-dipole *effective* radius $r_{\text{eff}}^2(r_1, r_2)$ is defined [17] in such a way to satisfy *color transparency*, namely $\sigma_{dd} \propto r_{i=1,2}^2$ when $r_i \rightarrow 0$. As in [17], three scenarios for $r_{\text{eff}}^2(r_1, r_2)$ will *a priori* be considered:

$$\mathbf{1.} \ r_{\text{eff}}^2 = \frac{r_1^2 r_2^2}{r_1^2 + r_2^2} \quad \mathbf{2.} \ r_{\text{eff}}^2 = \min(r_1^2, r_2^2) \quad \mathbf{3.} \ r_{\text{eff}}^2 = \min(r_1^2, r_2^2) \left\{ 1 + \ln \frac{\max(r_1, r_2)}{\min(r_1, r_2)} \right\}. \quad (5)$$

All three parametrisations exhibit *color transparency*. Cases **1** and **2** reduce to the original GBW model when one of the dipoles is much larger than the other and the model **3** corresponds to the dipole-dipole cross-section mediated by a two-gluon exchange [12]. For the saturation radius $R_0(\Delta\eta)$ we adopt the same set of parameters³ as those in [8, 17].

III. HARD CROSS-SECTIONS

Let us derive the general formulae we get for the cross-sections (1). Defining $u = r_2/r_1$ and $r_{\text{eff}}^2 = r_1^2 f_i(u)$, the three scenarios considered in (5) can be rewritten

$$f_1(u) = \frac{u^2}{1+u^2} \quad f_2(u) = \begin{cases} u^2 & \text{if } u < 1 \\ 1 & \text{if } u > 1 \end{cases} \quad f_3(u) = \begin{cases} u^2(1 - \log u) & \text{if } u < 1 \\ 1 + \log u & \text{if } u > 1 \end{cases}. \quad (6)$$

Then inserting (3) in formula (1) leads to

$$\begin{aligned} \frac{\sigma_i}{\sigma_0} &= 1 - Q_1 Q_2 \int_0^\infty du \int_0^\infty r dr J_1(rQ_1) J_1(ruQ_2) e^{-\frac{r^2}{4R_0^2} f_i(u)} \\ &= 1 - 2R_0^2 Q_1 Q_2 \int_0^\infty \frac{du}{f_i(u)} e^{-(Q_1^2 + Q_2^2 u^2) R_0^2 f_i^{-1}(u)} I_1\left(\frac{2Q_1 Q_2 u R_0^2}{f_i(u)}\right), \end{aligned} \quad (7)$$

¹ This formula can also be obtained [15] for $\phi(r, z, Q^2)$, taking into account the energy fraction z shared between the quark and the antiquark of the dipole. However, since the dipole-dipole cross-sections we will consider are z -independent, we only have to consider the distributions ϕ integrated over z .

² For our purpose, we shall only use a high-energy approximation of the expressions quoted by the authors [17].

³ $\lambda = .288$, $\Delta\eta_0 = 8.1$ for $Q_0 \equiv 1 \text{ GeV}$.

after integration over r . I_1 is the modified Bessel function of the first kind. Formula (7) gives the theoretical cross-sections within the GBW model for hard hadronic probes.

Let us discuss our results. The dipole distribution $\phi(r, Q^2)$ is not everywhere positive but this is not *a priori* an obstacle as long as the corresponding total cross-sections (1) stay positive. This is for instance realized by the BFKL cross-section [15]. It is compulsory to verify whether or not this positivity is altered by saturation. By numerical inspection of formulae (7), we checked that the positivity constraint is verified. Qualitatively, this is due to the fact that the negative values of the Bessel functions in (7) are present for large dipole sizes whose contributions are strongly reduced by saturation.

Another constraint is to check that the cross-sections $\sigma_{dd} \sim \sigma_0 r_{\text{eff}}^2/4R_0^2(\Delta\eta)$ corresponding to the limit of small dipole sizes in (4), lead to cross-sections behaving like $1/\{R_0^2(\Delta\eta) \max(Q_1^2, Q_2^2)\}$, as expected from transparency. Computing the gluon-gluon cross-section in this limit gives

$$\sigma_1 \sim \frac{\sigma_0}{R_0^2} \frac{2Q_1^2 Q_2^2}{(Q_1^2 + Q_2^2)^3} \quad \sigma_2 \sim \frac{\sigma_0}{R_0^2} \delta(Q_1^2 - Q_2^2) \quad \sigma_3 \sim \frac{\sigma_0}{2R_0^2} \min\left(\frac{1}{Q_1^2}, \frac{1}{Q_2^2}\right) \quad (8)$$

which shows that the models **1** and **3** of (5) verify the constraint. The model **2** does not, as confirmed by an explicit integration of (7) which gives in this case

$$\frac{\sigma_2}{\sigma_0} = e^{-R_0^2(Q_1^2 + Q_2^2)} I_0(2R_0^2 Q_1 Q_2) \sim \frac{e^{-R_0^2(Q_1 - Q_2)^2}}{2R_0 \sqrt{\pi Q_1 Q_2}} \rightarrow \frac{\delta(Q_1^2 - Q_2^2)}{R_0^2}, \quad (9)$$

at large R_0 . Hence, within our approximations, the model **2** cannot be considered.

It is possible to derive a general formula for saturation in the dipole framework which could be valid for any hard probe expressed in terms of the dipole basis, be it a forward jet, an onium, a virtual photon, etc... In particular, it will be useful to extend the saturation discussion to forward jets at HERA, with a $\gamma^* - g^*$ cross-section. We consider the Mellin transforms of the dipole distributions $\tilde{\phi}(\tau) = \int d^2r (r^2 Q^2)^\tau \phi(r, Q^2)$. For instance, one has

$$\tilde{\phi}(\tau) = 4^\tau \frac{\Gamma(1 + \tau)}{\Gamma(1 - \tau)} \quad \tilde{\phi}^\gamma(\tau) \propto \pi 2^{2\tau+1} \frac{\Gamma(1 - \tau)\Gamma(3 - \tau)\Gamma(\tau)\Gamma^2(1 + \tau)\Gamma(2 + \tau)}{\Gamma(4 - 2\tau)\Gamma(2 + 2\tau)}. \quad (10)$$

After some straightforward algebra, we obtain the following inverse Mellin transform expressions:

$$\frac{\sigma_i}{\sigma_0} = \int \frac{d\tau}{2i\pi} \tilde{\phi}^{(1)}(\tau) (2Q_1 R_0)^{-2\tau} \int \frac{d\sigma}{2i\pi} \tilde{\phi}^{(2)}(\sigma) (2Q_2 R_0)^{-2\sigma} g_i(\sigma, \tau); \quad 0 < \text{Re}(\sigma), \text{Re}(\tau), \text{Re}(\sigma + \tau) < 1, \quad (11)$$

where $\tilde{\phi}^{(1)}$ and $\tilde{\phi}^{(2)}$ are the Mellin-transformed dipole distributions in the target and projectile and, for the different models (5), one has

$$g_1(\sigma, \tau) = \frac{\Gamma(1 - \tau - \sigma)\Gamma(\sigma)\Gamma(\tau)}{\Gamma(1 + \tau + \sigma)} \quad g_2(\sigma, \tau) = \frac{\Gamma(1 - \tau - \sigma)}{\sigma\tau} \quad (12)$$

$$g_3(\sigma, \tau) = -2^{-\tau-\sigma} \Gamma(-\tau - \sigma) \{e^{2\sigma} \sigma^{-1-\tau-\sigma} \Gamma(\tau + \sigma + 1, 2\sigma) + [\tau \iff \sigma]\}.$$

This formulation allows us to extend easily our computations to various cases. After easy transformations, one gets for the different GBW models

$$\frac{\sigma_1}{\sigma_0} = \int_0^\infty dx J_1(x) A^{(1)}(xQ_1 R_0) A^{(2)}(xQ_2 R_0); \quad A(x) = \int \frac{d\tau}{2i\pi} x^{-2\tau} \tilde{\phi}(\tau) \Gamma(\tau)$$

$$\frac{\sigma_2}{\sigma_0} = \int_0^\infty 2x dx e^{-x^2} B^{(1)}(2xQ_1 R_0) B^{(2)}(2xQ_2 R_0); \quad B(x) = \int \frac{d\tau}{2i\pi} x^{-2\tau} \frac{\tilde{\phi}(\tau)}{\tau} \quad (13)$$

$$\frac{\sigma_3}{\sigma_0} = \frac{\sigma_2}{\sigma_0} + \int_0^\infty 2x dx e^{-x^2} \left(C^{(1)}(2xQ_1 R_0) D^{(2)}(2Q_2 R_0, x) + D^{(1)}(2Q_1 R_0, x) C^{(2)}(2xQ_2 R_0) \right)$$

where

$$C(x) = \int \frac{d\tau}{2i\pi} x^{-2\tau} \tilde{\phi}(\tau); \quad D(Q, x) = \int \frac{d\tau}{2i\pi} (Qx)^{-2\tau} \frac{\tilde{\phi}(\tau)}{\tau(2\tau + x^2)}. \quad (14)$$

With these general formulae, we find back our previous results (7,9) and obtain⁴ those for γ^* .

⁴ Note that the input functions A, B, C, D (13,14) correspond to specific Meijer functions.

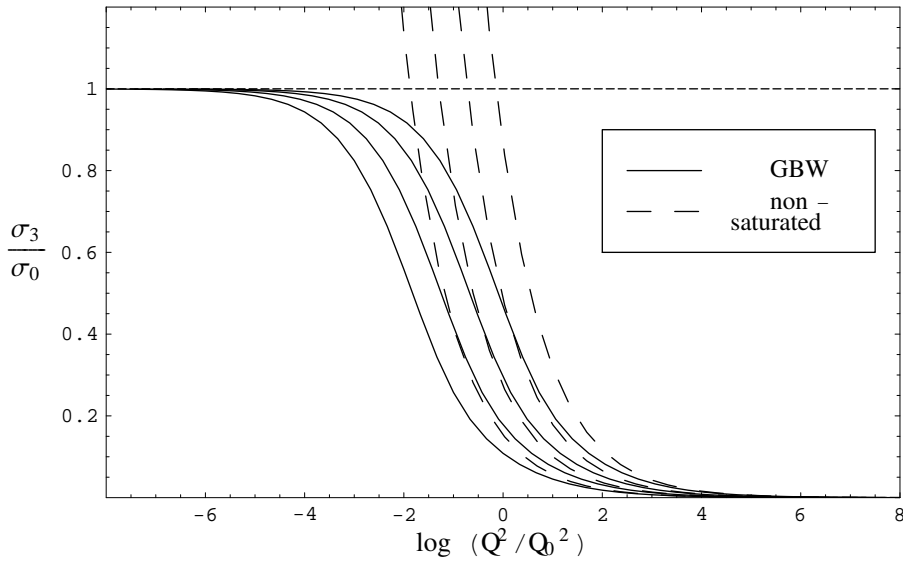


FIG. 2: $g^* - g^*$ cross-sections (model **3**). $Q_1 = Q_2 = Q$: symmetric virtuality case. $\Delta\eta =$ (from left to right) 4, 6, 8, 10 : rapidity intervals. Full lines: saturation cross-sections (7). Dashed lines: without saturation (8).

IV. PHENOMENOLOGICAL APPLICATIONS

Let us investigate the phenomenological outcome, for hadron colliders, of our extension of the GBW models to hadronic (*i.e.* g^*) probes. The theoretical cross-sections are obtained from formulae (6)-(7) and (11)-(14), in terms of the physical variables Q_1, Q_2 and $\Delta\eta$, once the saturation scale parameters Q_0, λ and $\Delta\eta_0$ are taken identical to their reference values (see footnote 3).

In Fig.2, we display the cross-section ratio σ_3/σ_0 as a function of $\log(Q^2/Q_0^2)$, where $Q = Q_1 = Q_2$ for values of the rapidity interval $\Delta\eta = 4, 6, 8, 10$. We also compare with the corresponding ratio for the non-saturated case (8). As expected, the curves show the well-known trend of the GBW model, namely a suppression of the non-saturated cross-sections, with a convergence towards the full saturation limit $\sigma \rightarrow \sigma_0$. In order to appreciate more quantitatively the influence of saturation, it is most convenient to consider the quantities $\mathcal{R}_{i/j}$ defined as

$$\mathcal{R}_{i/j} \equiv \frac{\sigma(Q_1, Q_2, \Delta\eta_i)}{\sigma(Q_1, Q_2, \Delta\eta_j)}, \quad (15)$$

i.e. the cross-section ratios for two different values of the rapidity interval. These ratios display in a clear way the saturation effects. They also correspond to possible experimental observables since they can be obtained from measurements at fixed values of the virtual gluon light-cone momentum and thus are independent of the gluon structure functions of the incident hadrons. Indeed, such observables have been used for a study of Mueller-Navelet jets for testing BFKL predictions at the Tevatron [22, 23, 24].

In Fig.3 we plot the values of $\mathcal{R}_{4.6/2.4}$ (resp. $\mathcal{R}_{8/4}$) as a function of $Q_1 = Q_2 \equiv Q$. These ratios correspond to values for Mueller-Navelet jets studied at the Tevatron [22, 23] (resp. realistic for the LHC [24]). The results are displayed both for models **1** and **3**, see (5).

As expected from the larger rapidity range, the decrease of \mathcal{R} between the transparency regime and the saturated one is larger for the LHC than for the Tevatron. The striking feature of Fig.3 is that the effect of saturation appears as a sharp transition for some critical range in Q (higher for the LHC).

Let us compare the resulting ratios for hadronic probes (g^* -initiated) to those for the virtual photon (γ^* -initiated) for the same values of the rapidity ranges, see Fig.3. Interestingly enough, the photon transition curve is much smoother, a phenomenon which can be explained by the different structure of the dipole distribution function. Indeed, as discussed previously [15], the dipole distribution $\phi(r, Q^2)$ has a tail extending towards large dipole sizes, which are more damped by the saturation corrections. Hence $\phi(r, Q^2)$ is more abruptly cut by saturation than the photon dipole distribution $\phi^\gamma(r, Q^2)$.

In Fig.4, we display the variation of $\mathcal{R}_{8/4}$, when one looks for asymmetric situations, *i.e.* $Q_1 > Q_2$. As seen from

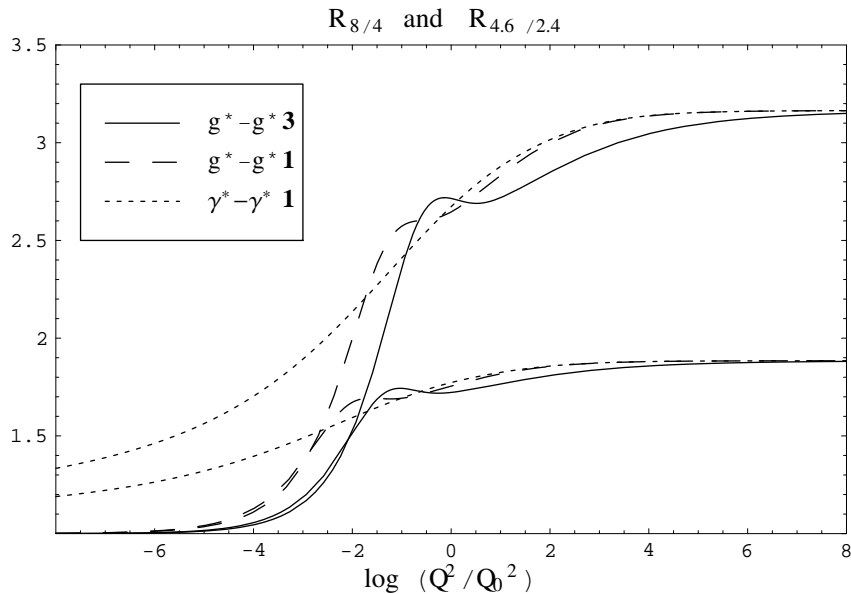


FIG. 3: *Cross-section ratios* $\mathcal{R}_{i/j}$. The resulting ratios for models **1** and **3** are plotted for rapidity intervals $i = 8, j = 4$ and $i = 4.6, j = 2.4$. The comparison is made with $\gamma^* - \gamma^*$ ratios for model **1** and equivalent kinematics. The non-saturated case would be a constant corresponding to the high Q^2 limit of the plots.

the figure, the transition may become even sharper in this case, with the formation of a bump at a rather high value of Q_1 , which could provide an interesting signal for the saturation scale. The origin of this bump lies in the different rate of increase of the cross-sections towards saturation when the virtualities are different. This possible signal is present at rather high scale, which could be useful for experimental considerations, as we shall develop now.

i) Mueller-Navelet jets

Two jets separated by a large rapidity interval, or Mueller-Navelet jets [10], are the more natural process for our formulae (7) to be applied. Indeed, a measurement of those dijet cross-sections has been performed at Tevatron, with jets of transverse momentum with a lower E_T cut, related to the virtuality Q . To actually measure the ratio \mathcal{R} in order to get rid of uncertainties on the structure functions, the two available incident energies (630 GeV and 1800 GeV) were used. The result was a strong increase of \mathcal{R} with the rapidity interval, which was pointed out as a possible hint of BFKL evolution. Saturation studies are favored by large rapidity intervals (as demonstrated in Fig.3). The relevant range of virtuality Q for expecting a clear saturation signal is albeit rather low (see Fig.3, 4).

If the strong experimental signal reported in [22] appears to be confirmed, the saturation prediction displayed in Fig.3 could well be relevant (with a redefinition of the parameters). However, the BFKL evolution itself at Tevatron energies appears to be quite sizeably modified by finite energy, running coupling corrections [25] and by experimental cuts [26]. Anyway, a simulation of Mueller-Navelet jets that would incorporate the relation between the E_T cut of the jet and the virtuality Q is needed to discuss the feasibility of saturation tests in this case.

ii) Heavy vector mesons

As an alternative to hard forward jets, one could consider [27] the detection of two heavy vector mesons with moderate transverse momentum and separated by large rapidity intervals. Indeed, using J/Ψ 's or Υ 's may provide a hadronic probe of precise mass and transverse momentum. It potentially realizes a colorless $q\bar{q}$ probe and thus could give an information on the differential distribution of dipoles $\phi(r, Q^2)$, for instance on the dipole-size distribution. Moreover, the leptonic decays may facilitate the event selection.

iii) Charmed and beauty hadrons

A forward-jet detection corresponds to one of the $q\bar{q}$ partners of a dipole. The detection of a heavy flavored meson would give a similar interesting signal. One thus would look for the detection of heavy flavored mesons separated by a large rapidity interval. In particular, the detection of a D^* on one side and a B -meson on the other side would realize

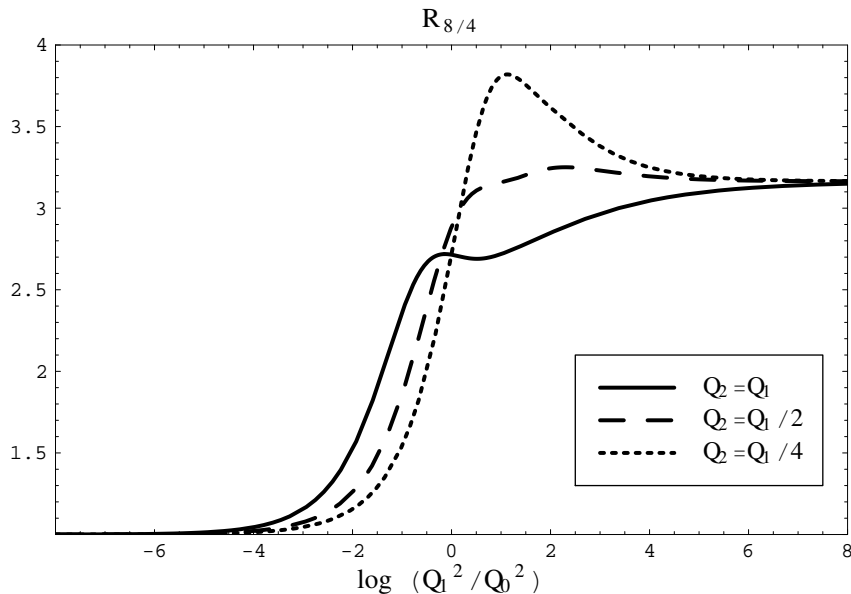


FIG. 4: $\mathcal{R}_{8/4}$, *asymmetric case*. The curves are drawn for model **3**. Note the bump at $Q_1^2/Q_0^2 \sim 3$.

interesting asymmetric configurations⁵ such as seen on Fig.4. One could also play with their transverse momentum cuts to vary the g^* virtualities.

These possibilities of realizing hadronic probes of saturation certainly deserve more studies in the near future. Simulations of these processes at Tevatron and LHC energies will give a quantitative estimate of the potential of hadronic colliders to reveal new features of saturation.

V. CONCLUSION AND OUTLOOK

Let us briefly summarize the main results of our study.

We started from an extension of the Golec-Biernat and Wüsthoff saturation model to hadronic collisions. For this sake, we used a QCD dipole formulation [15, 16] of hard hadronic probes based on a k_T -factorization assumption; such probes as forward (Mueller-Navelet) jets, heavy mesons, heavy flavoured mesons are initiated by off-mass-shell gluons. Our results are:

i) A derivation of saturation predictions for total hard cross-sections at hadron colliders, *e.g.* the Tevatron and LHC.

ii) Observables which possess a potentially clear signal for saturation at high rapidity intervals and gluon virtualities around the expected saturation scale in dipole-dipole interactions, see Figs.(2-4).

iii) The suggestion of using, besides the well-known Mueller-Navelet jets, heavy vector and/or heavy flavoured mesons to measure hard cross-sections and their transition towards saturation.

There are quite a few open issues for the present formalism:

On a phenomenological ground, it indicates a way for simulations in the framework of hadron colliders using the QCD dipole formalism which had been so useful in the HERA context. These phenomenological studies will tell us whether and how saturation could be present and checked at the Tevatron and/or the LHC. Note also that forward jets at HERA, which are initiated by $g^* - \gamma^*$ configurations with large rapidity separation, could be interesting to investigate. Beyond the scope of the present paper, determinant experimental issues, like fighting against pile-up events, background studies, possibility of a direct access to the hard cross-section ratios $\mathcal{R}_{i/j}$, etc... deserve to be explored.

⁵ Note that asymmetric configurations are preferable to avoid eventual non-BFKL logarithmic corrections [26].

On the theoretical ground, a study going beyond the single $q\bar{q}$ basis for the hard probe dipole distribution is deserved. In particular, adding the $gq\bar{q}$ or few-dipole configurations is important to discuss the k_T -factorization assumption. A more complete study of saturation effects in the emission of an energetic gluon [19] deserves further investigation. It may also allow us to extend our formalism to diffraction processes, since such configurations appeared important for the GBW model [8] at HERA. It is also possible to extend the theoretical analysis beyond the GBW formulation and to directly introduce solutions [28] of the non-linear QCD evolution equations, which would have a BFKL (and not merely transparency) limit at low density.

Acknowledgments

We thank Rikard Enberg, Christophe Royon and Stéphane Munier for useful comments and suggestions.

-
- [1] L. N. Lipatov, *Sov. J. Nucl. Phys.* **23**, (1976) 338; E. A. Kuraev, L. N. Lipatov and V. S. Fadin, *Sov. Phys. JETP* **45**, (1977) 199; I. I. Balitsky and L. N. Lipatov, *Sov. J. Nucl. Phys.* **28**, (1978) 822.
 - [2] L. V. Gribov, E. M. Levin and M. G. Ryskin, *Phys. Rep.* **100**, (1983) 1.
 - [3] A. H. Mueller and J. Qiu, *Nucl. Phys.* **B268**, (1986) 427.
 - [4] L. McLerran and R. Venugopalan, *Phys. Rev.* **D49**, (1994) 2233; *ibid.*, (1994) 3352; *ibid.*, **D50**, (1994) 2225; A. Kovner, L. McLerran and H. Weigert, *Phys. Rev.* **D52**, (1995) 6231; *ibid.*, (1995) 3809; R. Venugopalan, *Acta Phys. Polon.* **B30**, (1999) 3731; E. Iancu, A. Leonidov and L. McLerran, *Nucl. Phys.* **A692**, (2001) 583; *Phys. Lett.* **B510**, (2001) 133; E. Iancu and L. McLerran, *Phys. Lett.* **B510**, (2001) 145; E. Ferreira, E. Iancu, A. Leonidov and L. McLerran, *Nucl. Phys.* **A703**, (2002) 489; H. Weigert, *Nucl. Phys.* **A703**, (2002) 823.
 - [5] I. Balitsky, *Nucl. Phys.* **B463**, (1996) 99; Y. V. Kovchegov, *Phys. Rev.* **D60**, (1999) 034008; *ibid.*, **D61**, (2000) 074018.
 - [6] E. Levin and J. Bartels, *Nucl. Phys.* **B387**, (1992) 617; Y. V. Kovchegov, *Phys. Rev.* **D61**, (2000) 074018; E. Levin and K. Tuchin, *Nucl. Phys.* **A693**, (2001) 787; *ibid.*, **A691**, (2001) 779.
 - [7] A. H. Mueller and D. N. Triantafyllopoulos, *Nucl. Phys.* **B640**, (2002) 331.
 - [8] K. Golec-Biernat and M. Wüsthoff, *Phys. Rev.* **D59** (1998) 014017, *Phys. Rev.* **D60** (1999) 114023.
 - [9] G. Altarelli and G. Parisi, *Nucl. Phys.* **B126** 18C (1977) 298. V. N. Gribov and L. N. Lipatov, *Sov. Journ. Nucl. Phys.* (1972) 438 and 675. Yu. L. Dokshitzer, *Sov. Phys. JETP.* **46** (1977) 641. For a review: Yu. L. Dokshitzer, V. A. Khoze, A. H. Mueller and S. I. Troyan *Basics of perturbative QCD* (Editions Frontières, J. Tran Thanh Van Ed. 1991).
 - [10] A. H. Mueller and H. Navelet, *Nucl. Phys.* **B282** (1987) 727.
 - [11] N. N. Nikolaev and B. G. Zakharov, *Zeit. für. Phys.* **C49** (1991) 607; *Phys. Lett.* **B332** (1994) 184.
 - [12] A. H. Mueller, *Nucl. Phys.* **B415** (1994) 373; A. H. Mueller and B. Patel, *Nucl. Phys.* **B425** (1994) 471; A. H. Mueller, *Nucl. Phys.* **B437** (1995) 107.
 - [13] S. Munier and R. Peschanski, *Nucl. Phys.* **B524** (1998) 377. A. Bialas, H. Navelet and R. Peschanski, *Nucl. Phys.* **B593** (2001) 438.
 - [14] S. Catani, M. Ciafaloni and F. Hautmann, *Nucl. Phys.* **B366** (1991) 135. J. C. Collins and R. K. Ellis, *Nucl. Phys.* **B360** (1991) 3; E. M. Levin, M. G. Ryskin, Yu. M. Shabelsky and A. G. Shuvaev, *Sov. J. Nucl. Phys.* **53** (1991) 657.
 - [15] R. Peschanski, *Mod. Phys. Lett.* **A15** (2000) 1891.
 - [16] S. Munier, *Phys. Rev.* **D63** (2001) 034015.
 - [17] N. Timneanu, J. Kwieciński and L. Motyka, *Eur. Phys. J.* **C23** (2002) 513, *Acta Phys. Polon.* **B33** (2002) 1559 and 3045.
 - [18] F. Gélis and R. Venugopalan, *Large mass Q-Qbar production from the Color Glass Condensate*, hep-ph/0310090.
 - [19] Yu. V. Kovchegov, *Phys. Rev.* **D64** (2001) 114016; Yu. V. Kovchegov, K. Tuchin, *Phys. Rev.* **D65** (2002) 074026.
 - [20] J. Kwiecinski, A. D. Martin and P. J. Sutton, *Phys. Rev.* **D52** (1995) 1445.
 - [21] H. Navelet and S. Wallon, *Nucl. Phys.* **B522** (1998) 237.
 - [22] D0 Collaboration: B. Abbott, *et al*, *Phys. Rev. Lett.* **84** (2000) 5722.
 - [23] J. G. Contreras, R. Peschanski and C. Royon, *Phys. Rev.* **D62** (2000) 034006.
 - [24] R. Peschanski and C. Royon, *Pomeron intercepts at colliders*, Workshop on physics at LHC, hep-ph/0002057.
 - [25] L. H. Orr and W. J. Stirling, *Phys. Lett.* **B429** (1998) 135.
 - [26] J. R. Andersen, V. Del Duca, S. Frixione, C. Schmidt and W. J. Stirling, *JHEP* **0102** (2001) 007.
 - [27] C. Royon, private communication.
 - [28] E. Iancu, K. Itakura and S. Munier, *Saturation and BFKL dynamics in the HERA data at small x*, hep-ph/0310338.